

Supplementary data

Three sources of CO₂ were used in the experiments: hydrous oxalic acid, H₂C₂O₄•2H₂O (HOX), silver oxalate, AgCO₂, (AgOX), and silver carbonate (Ag₂CO₃). For fluid mixtures up to X_{CO_2} of 0.5, reagent HOX was used with varying amounts of H₂O. The HOX (Fisher Certified) is in the form of limpid crystals of about 10 µg, which could be loaded individually to achieve a desired fluid mass. This material generates a fluid mix of molar proportions 2H₂O:2CO₂:H₂ during an experiment. The H₂ must be purged by buffering at high oxygen fugacity (f_{O_2}). Experiments in this laboratory and elsewhere (Rosenbaum and Slagel 1995) have shown that HOX reliably generates a 50 mol % CO₂ mixture with H₂O if buffered externally with hematite-magnetite-H₂O, with the Pt capsule acting as a H₂-permeable membrane. The principal disadvantage of this method is that a welded Pt inner capsule must be used to contain the experimental charge, since most of the large capsule volume is filled with the buffer mix (totaling about 100 mg). This limits the CO₂-H₂O fluid mass to only about 5 mg and the crystal mass to 0.5 mg. For high CO₂ fluids the quartz weight loss would be too small to measure with the buffered capsule method.

Experiments with >50 mol % CO₂ used AgOX as a CO₂ source. AgOX is a conveniently loaded material (small coherent pellets of powder), but it decomposes at low T and cannot be oven dried. Previous work in this laboratory (Ferry et al. 2002) has shown that our material (ICN batch #23962-A) has a small amount of adsorbed H₂O, and, moreover, the slightly gray color indicates probable slight photodecomposition to Ag metal. For these reasons the volatile yield of AgOX had to be calibrated by weight loss measurements. An aliquot of about 50 mg of AgOX with or without additional H₂O was

weighed into a segment of the large Pt tube and welded without significant mass loss. This charge was run at the same conditions as all experiments (800 °C, 10 kbar) for periods of up to two days and quenched in the usual manner. The retrieved capsules were inflated due to CO₂ pressure and showed no mass loss. A capsule was punctured with a tiny hole under liquid N₂ using a sharp needle, and then placed in a refrigerator freezer for up to one hour. This procedure is necessary to avoid spraying of liquid H₂O upon puncture. The capsule was weighed at intervals until a constant weight (the “plateau weight”, Table S1) was attained, which usually took about 1/2 hr. Comparison weighings with liquid H₂O showed that the puncture hole was too small to allow weighable evaporation of liquid water at room temperature. The plateau weight was taken to indicate, by subtraction, the CO₂ yield. The perforated capsule was then heated at 115 °C for 15 minutes followed by 15 minutes at 350 °C. The additional weight loss was taken as the total H₂O yield. Four such volatile loss experiments were performed (Table S1). The runs consistently showed that a small fraction of the expected volatile yield of the AgOX was actually H₂O. They also revealed a small additional CO₂ mass deficiency, which presumably results from photodecomposition. A typical gas yield analysis is shown in Fig. S1. The four yield tests were averaged to obtain corrected CO₂ and H₂O yields: 95.5 wt% of the expected CO₂ yield, based on AgCO₂ stoichiometry, and 2.79 wt% of the expected CO₂ yield, respectively.

A third starting fluid source consisted of silver carbonate (Ag₂CO₃: Aesar 99.999% certified) and HOX in equimolar proportions, so that the excess H₂ of the HOX and the excess O of the Ag₂CO₃ were compensated. A serious disadvantage of this CO₂ source is the very large amount of Ag and the relatively small amount of CO₂ yielded by

the Ag_2CO_3 . For reasons not clear, the quartz crystals sometimes became coated with Ag metal and could not be easily cleaned. A few runs were made with the quartz crystal protected by a perforated inner Pt capsule, but in these experiments the perforations were plugged by Ag metal, and the crystals yielded anomalously low weight losses compared to results based on other methods. These manifestly underequilibrated runs are not reported in Table 1, text. Thus, the $\text{Ag}_2\text{CO}_3 + \text{HOX}$ mix was less satisfactory as a CO_2 source at high CO_2 mole fractions.

Activities of H_2O and SiO_2 from this study and others at different P and T are tabulated in Table S2, and plotted in Fig. 2C, text.

References cited

- Anderson, G.M. and Burnham, C.W (1965) The solubility of quartz in supercritical water. *American Journal of Science*, 263, 494–511.
- Ferry, J.M., Newton, R.C. and Manning, C.E. (2002) Experimental determination of the equilibria: rutile + magnesite = geikielite + CO_2 and zircon + 2magnesite = baddeleyite + forsterite + 2CO_2 . *American Mineralogist*, 87, 1342–1350.
- Rosenbaum, J.M. and Slagel, M.M. (1995) C-O-H speciation in piston-cylinder experiments. *American Mineralogist*, 80, 109–114.

Figure caption

Figure S1. Volatile yield from silver oxalate decomposition in a welded Pt capsule at 800 °C and 10 kbar (Run 32, Table S1). The quenched, inflated capsule was punctured under liquid N_2 and left in a freezer for 1 hr before weighing began.

Table S1. Volatile yields of silver oxalate (AgOX).

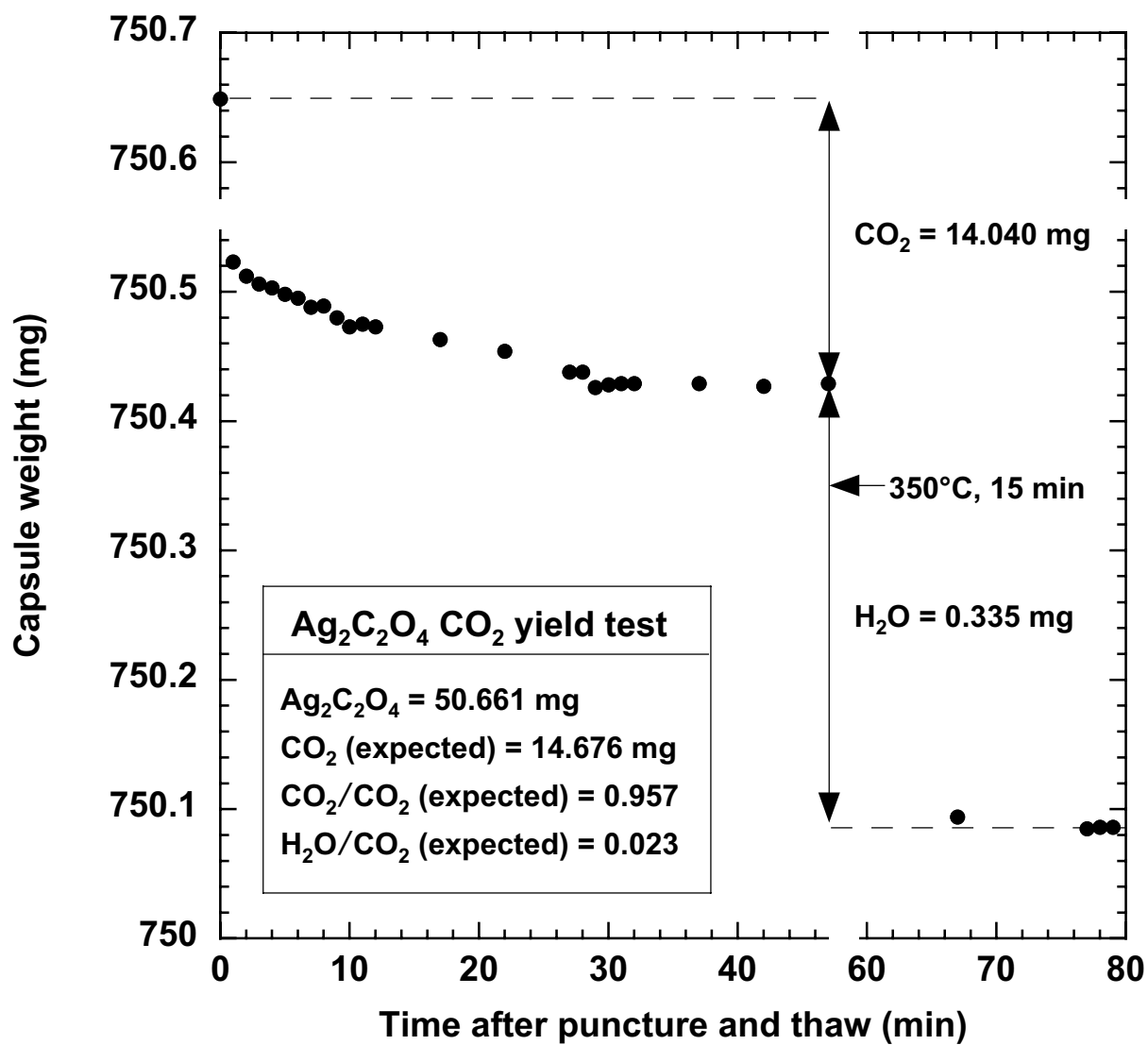
Expt. no.	Run Time (hr)	AgOX (mg)	H ₂ O (mg)	Capsule Out (mg)	Capsule change (mg)	Plateau weight (mg)	Dried Weight (mg)	% CO ₂ (of nom- inal CO ₂)	% H ₂ O (of nom- inal CO ₂)
32	8	50.661		764.469	-0.020	750.427	750.086	95.66(2)	2.32(2)
33	13	46.887		713.761	-0.028	700.873	700.396	94.86(2)	3.51(2)
34	9	46.260		732.112	-0.043	719.312	718.950	95.49(2)	2.70(2)
42	40	51.842	1.961	955.046	+0.005	940.620	938.262	96.03(2)	2.64(3)
Ave:								95.51(24)	2.79(25)

Weighing uncertainty is 2 μ g (1 σ); parenthetical entries are 1 σ or 1 standard error in last digit(s).

Table S2. Parameters derived from selected experimental studies of quartz solubility in H₂O-CO₂.

$X_{\text{H}_2\text{O}}$	$\log a_{\text{H}_2\text{O}}$	X_{SiO_2}	γ_{SiO_2}	a_{SiO_2}	$\log \frac{a_{\text{SiO}_2}}{a'_{\text{SiO}_2}}$	Notes
Novgorodov (1975), 700°C, 5 kbar, $K_{md} = 242$						
1	0	7.12E-03	0.413	2.94E-03	0	
0.91	-0.036	4.60E-03	0.482	2.22E-03	-0.122	
0.88	-0.046	3.94E-03	0.508	2.00E-03	-0.167	
0.87	-0.050	3.23E-03	0.541	1.75E-03	-0.225	
0.81	-0.071	2.61E-03	0.578	1.51E-03	-0.290	
0.72	-0.104	1.79E-03	0.643	1.15E-03	-0.408	
0.55	-0.181	6.62E-04	0.796	5.27E-04	-0.746	
0.527	-0.194	6.70E-04	0.795	5.33E-04	-0.742	
0.513	-0.202	7.50E-04	0.779	5.84E-04	-0.701	
0.503	-0.208	5.58E-04	0.819	4.57E-04	-0.808	
0.50	-0.210	5.28E-04	0.826	4.36E-04	-0.829	
0.495	-0.213	5.26E-04	0.826	4.34E-04	-0.830	
0.32	-0.359	2.60E-04	0.898	2.33E-04	-1.100	
Novgorodov (1975), 700°C, 3 kbar, $K_{md} = 309$						
1	0	4.79E-03	0.436	2.09E-03	0	From AB65
0.91	-0.036	2.79E-03	0.525	1.47E-03	-0.154	
0.77	-0.090	1.39E-03	0.643	8.97E-04	-0.367	
0.50	-0.225	3.70E-04	0.839	3.11E-04	-0.828	+graphite
0.36	-0.339	1.74E-04	0.911	1.58E-04	-1.120	+graphite
0.33	-0.371	1.51E-04	0.921	1.39E-04	-1.176	
0.23	-0.507	9.07E-05	0.949	8.61E-05	-1.385	+graphite
Walther and Orville (1983), 600°C, 2 kbar, $K_{md} = 250$						
1	0	2.17E-03	0.604	1.31E-03	0.000	From AB65
0.977	-0.010	1.91E-03	0.626	1.19E-03	-0.040	
0.964	-0.015	1.67E-03	0.649	1.08E-03	-0.083	
0.902	-0.039	1.25E-03	0.696	8.73E-04	-0.176	
0.889	-0.044	1.20E-03	0.703	8.43E-04	-0.191	
0.837	-0.063	9.49E-04	0.740	7.02E-04	-0.271	
0.702	-0.115	4.70E-04	0.836	3.93E-04	-0.523	
0.689	-0.121	3.81E-04	0.859	3.27E-04	-0.602	
Shmulovich et al (2001), 800°C, 9 kbar $K_{md} = 252$						
1	0	2.16E-02	0.261	5.63E-03	0	From S06
0.7027	-0.102	4.47E-03	0.443	1.98E-03	-0.455	
0.6482	-0.121	3.35E-03	0.482	1.62E-03	-0.542	
0.4991	-0.189	1.86E-03	0.555	1.03E-03	-0.737	
0.4992	-0.189	1.53E-03	0.588	9.02E-04	-0.796	
0.8354	-0.059	8.87E-03	0.355	3.15E-03	-0.253	
This study, 800°C, 10 kbar, $K_{md} = 229$						
1	0	2.20E-02	0.269	5.92E-03	0	From NM00
0.9234	-0.030	1.46E-02	0.319	4.54E-03	-0.116	
0.8216	-0.062	8.53E-03	0.394	3.18E-03	-0.270	
0.8163	-0.064	8.96E-03	0.387	3.27E-03	-0.257	
0.6663	-0.111	3.83E-03	0.522	1.84E-03	-0.509	
0.6599	-0.113	4.05E-03	0.513	1.90E-03	-0.493	
0.5748	-0.145	3.21E-03	0.552	1.59E-03	-0.571	
0.5002	-0.180	1.81E-03	0.650	1.05E-03	-0.753	
0.5000	-0.181	1.72E-03	0.658	1.01E-03	-0.768	
0.4435	-0.213	1.27E-03	0.709	7.94E-04	-0.873	
0.4379	-0.217	1.09E-03	0.732	7.11E-04	-0.920	
0.3696	-0.266	6.49E-04	0.807	4.65E-04	-1.105	
0.3180	-0.314	4.26E-04	0.857	3.26E-04	-1.259	
0.2528	-0.391	1.88E-04	0.926	1.59E-04	-1.570	

Abbreviations: AB65, Anderson and Burnham (1965); NM00, Newton and Manning (2000); S06, Shmulovich et al (2006). K_{md} calculated using Eq. 5, text.



Newton & Manning, Fig. S1